Polymer 50 (2009) 2944–2952

Contents lists available at ScienceDirect

Polymer

journal homepage: www.elsevier.com/locate/polymer

Photochemical and photophysical reactions of poly(propylene imine) dendrimers tethering cinnamamide groups

Seiichi Furumi [a,b,*], Akira Otomo [b], Shiyoshi Yokoyama [b,c], Shinro Mashiko [b]

[a] National Institute for Materials Science (NIMS), 1-2-1 Sengen, Tsukuba, Ibaraki 305-0047, Japan
[b] National Institute of Information and Communications Technology (NICT), 588-2 Iwaoka, Nishi-ku, Kobe 651-2492, Japan
[c] Institute for Materials Chemistry and Engineering (IMCE), Kyushu University, 6-1 Kasuga-koen, Kasuga, Fukuoka 816-8580, Japan

ARTICLE INFO

Article history:
Received 16 January 2009
Received in revised form
8 April 2009
Accepted 22 April 2009
Available online 3 May 2009

Keywords:
Dendrimers
Energy transfer
Phosphorescence

ABSTRACT

Here we report on photochemical and photophysical properties of poly(propylene imine) dendrimers tethering cinnamamide groups at the peripheral positions. Photoexcitation of the dendrimer solutions with 313 nm brought about monotonous decrease of absorption band of *trans*-cinnamamide around 270 nm as a result of *trans*-to-*cis* photoisomerization and [2+2] photocycloaddition. The first-generation dendrimer showed preferential formation of *cis*-isomer, whereas photocycloaddition was more favorable for the third- and fifth-generation dendrimers. Interestingly, the third- and fifth-generation dendrimers could encapsulate phosphorescent donors into the dendrimer nanocavities. When the dendrimers capturing the donors were excited at 365 nm, photocycloaddition proceeded efficiently through triplet–triplet energy transfer. By analyzing phosphorescence spectra with theoretical Perrin's formula, we found that this triplet–triplet energy transfer is quenched within a radius of ~0.5 nm. Such triplet–triplet energy transfer within dendrimer nanocavities would provide promising strategy to design and fabricate novel molecular devices by utilizing the dendrimers.

1. Introduction

Molecular interactions between ground and excited states of organic chromophores have been a long-standing subject of considerable interest [1]. Among these interactions, excited energy or electron transfers from excited donor to acceptor species are crucial photophysical events in molecular assemblage systems. In particular, energy transfer (ET) plays a considerable role not only in the natural phenomenon of photosynthesis [2], but also in the technological advancement of the performance of organic light-emitting diodes (OLEDs) [3]. This kind of process takes place not only by a radiative process through the absorption of emitted photon, but also by a non-radiative process. Moreover, the latter process is divided into two mechanisms: singlet–singlet energy transfer by dipole–dipole interaction (S-ET: Förster transfer) [4] and triplet–triplet energy transfer by electron exchanges (T-ET: Dexter transfer) [5]. The rate constants (k_{ET}) for S-ET and T-ET process can be described by the following equations:

$$\text{S-ET(Förster transfer)} : k_{ET}(\text{Förster}) \approx \left[(f_D f_A)/\nu^2 R_{DA}^6\right] J \quad (1)$$

$$\text{T-ET(Dexter transfer)} : k_{ET}(\text{Dexter}) \approx e^{-2R_{DA}/L} J \quad (2)$$

where f_D and f_A mean the oscillator strengths of the donor and acceptor transition, respectively. L is a constant related to an effective average orbital radius; J, the spectral overlap integral; and R_{DA}, the distance between the donor and the acceptor. According to Eq. (1), the rate of S-ET decreases with R_{DA}^{-6}. Therefore, the transfer range in S-ET can reach 10 nm due to dipole–dipole interaction.

On the other hand, T-ET by electron exchanges is a very important type of energy transfer observed in diffusion-controlled conditions such as rigid solutions and glassy solid states [1b,5]. This is because the T-ET process requires electrical collisions between donor and acceptor during the relatively long lifetime of the donor at triplet excited state. Consequently, T-ET takes place within typically short range of 0.3–1.0 nm. This phenomenon follows Eq. (2). Therefore, the T-ET rate decreases *exponentially* with $-2R_{DA}$. This process is strongly dependent on the distance between donor and acceptor on nanometer scale. Recent advances in the OLED research realm have facilitated the enhancement of the light-emitting efficiency by utilizing the photophysical T-ET process [3].

In this context, dendrimers have been attracting currently considerable interests from photochemical and photophysical

* Corresponding author. National Institute for Materials Science (NIMS), 1-2-1 Sengen, Tsukuba, Ibaraki 305-0047, Japan. Tel.: +81 29 859 2468; fax: +81 29 859 2201.
E-mail address: furumi.seiichi@nims.go.jp (S. Furumi).

0032-3861/$ – see front matter
doi:10.1016/j.polymer.2009.04.039

viewpoints, because they are radically branched polymers with well-defined spherical shapes at nanometer scale [6]. By utilizing the intrinsic molecular structure, the intramolecular photoexcited S-ET process with dendrimers is a widely investigated research topic. The major concern of S-ET with dendrimers is the artificial organization of highly efficient light-harvesting antennas, similar to photosynthesis. On the other hand, to date, the research progress of photoexcited T-ET in dendrimers trails that of S-ET. This situation motivates us to evaluate the photoexcited T-ET process within dendrimers by taking note of the following features. First, the T-ET process takes place within scale of a few nanometers by electron exchanges of both highest occupied molecular orbitals (HOMOs) and lowest unoccupied molecular orbitals (LUMOs) between donor and acceptor according to Eq. (2). Secondly, high-generation dendrimers have an intrinsic property that organic dyes, nanoparticles and so forth are encapsulated in the internal dendrimer cavities with nanometer scales so as to prevent them from interacting with the surrounding molecules [7]. However, to the best of our knowledge, there are a few reports on photoisomerizations in dendrimers through the photoexcited T-ET [6c,8] or electron transfer process [9]. In contrast, we found preliminary data that show [2+2] photocycloaddition of *trans*-cinnamamide attached to dendrimers can proceed readily through the photoexcited T-ET process when phosphorescent donors are encapsulated into the dendrimer cavities [10]. The mechanism of spectral changes still remains obscure from photophysical viewpoint. This paper describes the details of the photochemical behaviors of poly(propylene imine) dendrimers tethering cinnamamide groups and the photophysical T-ET process by encapsulating the phosphorescent donors in the dendrimer cavities. By measurements and analyses of the absorption, phosphorescent and mass spectra, it was revealed that highly efficient photocycloaddition of dendrimers takes place through the photoexcited T-ET process in nanometer scale, as depicted in Fig. 1. In particular, the detailed analysis of phosphorescence spectra in combination with theoretical Perrin's formula revealed that the present T-ET process from the benzophenone donors is completely quenched by *trans*-cinnamamide acceptors within a radius of ~0.5 nm.

2. Experimental section

2.1. Synthesis of cinnamamide-terminated dendrimers

For the purpose of this study, we synthesized the first-, third- and fifth-generation poly(propylene imine) dendrimers (**G1**, **G3** and **G5**, respectively) covalently modified with photoreactive cinnamamide groups at the peripheral positions. The chemical structures are shown in Fig. 2. The first-, third- and fifth- generation poly(propylene imine) dendrimers were converted into photoreactive dendrimers through reaction with *trans*-cinnamamide chloride in the presence of triethylamine. The resultant dendrimers were purified by repetitive dialysis and reprecipitation to obtain a narrowed dispersion of molecular weights. The chemical structures were characterized by ^{1}H and ^{13}C NMR, electrospray ionization (ESI) mass, matrix assisted laser desorption/ionization-time of flight (MALDI-TOF) mass and size-exclusion chromatography (SEC) measurements. For comparison with photochemical properties of the dendrimers, *trans*-cinnamamide (**G0**) was used after recrystallization.

G1. ^{1}H NMR (300 MHz, $CDCl_3$, 23 °C, TMS) δ [ppm]: 1.45 (s, 4H, $NCH_2CH_2CH_2CH_2N$), 1.69 (m, 8H, $NCH_2CH_2CH_2N$), 2.43 (m, 12H, $NCH_2CH_2CH_2N$, $NCH_2CH_2CH_2CH_2N$), 3.43 (m, 8H, CH_2NHCO), 6.52 (d, J = 16 Hz, 4H, ArCH=CHCO), 7.26 (br, 4H, CONH), 7.27 (m, 12H, Ar-H), 7.28 (m, 8H, Ar-H), 7.46 (d, J = 16 Hz, 4H, ArCH=CHCO). MS calculated for $C_{52}H_{64}N_6O_4$: 836; (ESI, positive) found 837 $[M+H]^+$ and 859 $[M+Na]^+$.

G3. ^{1}H NMR (300 MHz, $CDCl_3$, 23 °C, TMS) δ [ppm]: 1.45–1.65 (br, 60H, $NCH_2CH_2CH_2CH_2N$, $NCH_2CH_2CH_2N$, $NCH_2CH_2CH_2NH$), 2.41–2.91 (br, 84H, $NCH_2CH_2CH_2N$, $NCH_2CH_2CH_2CH_2N$), 3.44 (br, 32H, CH_2NHCO) 6.52 (br, 16H, ArCH=CHCO), 7.02 (br, 16H, $CH{=}CHCONHCH_2$), 7.26–7.44 (br, 80H, Ar-H), 7.62 (d, J = 16 Hz, 16H, ArCH=CHCO). MS calculated for $C_{232}H_{304}N_{30}O_{16}$: 3768; (MALDI-TOF, positive) found 3769 $[M+H]^+$, 3808 $[M+K]^+$.

G5. ^{1}H NMR (600 MHz, $CDCl_3$, 23 °C, TMS) δ [ppm]: 1.41–1.78 (br, 252H, $NCH_2CH_2CH_2CH_2N$, $NCH_2CH_2CH_2N$, $NCH_2CH_2CH_2NH$), 2.32–3.43 (br, 500H, $NCH_2CH_2CH_2N$, $NCH_2CH_2CH_2CH_2N$, CH_2NHCO), 6.51–7.68 (br, 512H, ArCH=CHCO, $CH{=}CHCONHCH_2$, Ar-H). ^{13}C NMR (150 MHz, $CDCl_3$, 23 °C) δ [ppm]: 24.1 ($NCH_2CH_2CH_2CH_2N$, $NCH_2CH_2CH_2N$), 27.0 ($NCH_2CH_2CH_2NHCO$), 37.9 (CH_2CH_2NHCO), 51.1–51.9 ($N(CH_2)_3$), 121.6 (ArCH=CHCO), 127.8 (C-Ar), 128.8 (C-Ar), 129.5 (C-Ar), 134.9 (C-Ar), 140.2 (ArCH=CHCO), 166.8 (CO). IR (KBr) ν [cm^{-1}]: 3270 (N–H stretch), 3061 (sec. N–H stretch), 2943 (C–H sat.), 1662 (C=O (amide I)), 1616 (Ar and HC=CH), 1551 (N–H bend (amide II)).

2.2. General techniques and physical measurements

The synthesized dendrimers were characterized by ^{1}H NMR, ESI mass, MALDI-TOF mass and SEC measurements. ^{1}H NMR spectra

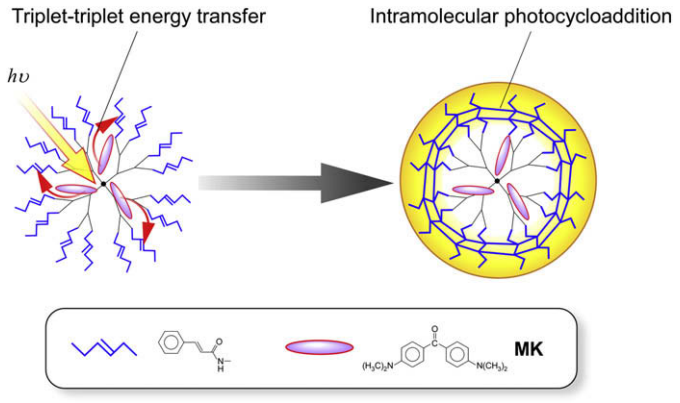

Fig. 1. Schematic research concept of photoinduced triplet–triplet energy transfer (T-ET) in dendrimer nanocavities leading to intramolecular photocycloaddition reaction. Blue zigzag lines denote cinnamamide units, and red ellipses are Michler's ketone (**MK**) molecules as phosphorescent donors.

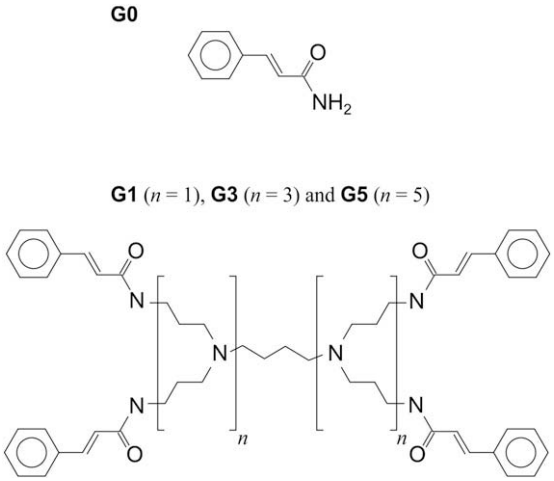

Fig. 2. Chemical structures of *trans*-cinnamamide (top, **G0**) and photoreactive dendrimers bearing *trans*-cinnamamides at the peripheral positions (bottom: **G1**, **G3** and **G5**).

were recorded on Fourier transform (FT) NMR spectrometers (JEOL, JNM-LA 300 or JNM-ECP 600) with tetramethylsilane (TMS) as an internal standard. ^{13}C NMR spectra were measured by FT-NMR spectrometer (Bruker BioSpin, DRX-600). Mass spectra were recorded on an ESI mass spectrometer (Bruker Daltonics, Esquire 3000) for **G1** and a MALDI-TOF mass spectrometer (Shimadzu, KRATOS MALDI IV time-delayed extraction) for **G3** and **G5**. FT-IR spectrum of **G5** was taken on an infrared spectrometer (Perkin–Elmer, Spectrum GX-Raman). SEC profile was recorded on a pump system (Waters, 600) equipped with a column (Waters, Styragel HR 3 with 100 nm pore size) and a tunable absorption detector (Waters, 486) using tetrahydrofuran as eluent. The molecular weights obtained from the SEC profile were calibrated on the basis of standard poly(styrene)s (Showa denko, Shodex SL-105; $M_w = 5.8 \times 10^2$ to 2.1×10^4). The thermal characteristics were evaluated using melting point apparatus (Yanaco, MP-S3). Molecular dynamics simulations (Molecular Simulations, Cerius^2) were carried out on the basis of DREIDING force field. SMART algorithm was employed to minimize the energy of molecular structures. The simulations did not contain effect of the surrounding solvents, providing thereby the molecular shape in vacuum environment.

Photoirradiation with UV light was performed using a 200 W Hg–Xe lamp (San-ei Electric MFG. CO., UV Supercure-203S) equipped with appropriate glass filters. The light intensity was measured using a power energy analyzer (Coherent, Field Master) equipped with a semi-conducting sensor (Coherent, Smart Sensors LM-2 UV). Electronic absorption spectra were recorded on a scanning spectrophotometer (Hitachi, U-4000). Phosphorescence spectra were measured using a scanning spectrofluorometer under nitrogen atmosphere (Hitachi, F-4500).

3. Results and discussion

3.1. Characterization of cinnamamide-terminated dendrimers

NMR, MS and SEC measurements of the synthesized dendrimers revealed nearly full modification of *trans*-cinnamamide residues at the termini of poly(propylene imine) dendrimers, as follows. Although **G1**, **G3** and **G5** appeared nearly identical in terms of their ^1H NMR spectra, we found that the resonant peaks broaden with an increase in the dendrimer generation. The cinnamamide groups were assigned to be thoroughly *trans*-isomer from the coupling constants of the alkene protons with 16 Hz in ^1H NMR spectra. We clearly observed the coupling constant of **G1** and **G3**. By mass spectral analysis, it was found that **G1** and **G3** show corresponding molecular weight in ESI and MALDI-TOF mass spectra, respectively. However, we could not obtain clear peak of **G5** not only in ESI, but also in MALDI-TOF mass spectrum. This probably happened because the difficulty in ionization of high molecular weights. Such observation is consistent with several precedent of poly(propylene imine) dendrimers tethering oligo(*p*-phenylene vinynele) or pyrene moieties [11]. Therefore, we measured ^{13}C NMR and FT-IR spectra of **G5**. The results are shown in Section 2 and Supplementary material (Fig. S1). SEC measurement was carried out in order to evaluate purity of the synthesized dendrimers. As compiled in Table 1, we found that the dendrimers exhibit relatively high purity.

Moreover, we carried out molecular simulation in order to obtain clues with regard to both the molecular shape of dendrimer and the steric crowding of cinnamamide units on the dendrimer surface. Fig. 3 shows the molecular models of **G1**, **G3** and **G5**. The molecular shape became spherical with an increase in the dendrimer generation. As can been seen from this model, it was found that the dendrimer backbones of **G3** and **G5** are blinded by the *trans*-cinnamamide groups settled at the dendrimer peripheral positions. The radii of gyration estimated from the molecular models were a few nanometers in scale (Table 1), and similar value of phenylalanine- and pyrene-functionalized poly(propylene imine) dendrimers [11b,12].

Table 1
Physical properties of photoreactive dendrimers bearing cinnamamide units.

	G1	G3	G5
M_w[a]	905	4103	16084
Calcd m/z	837	3768	15497
M_w/M_n[b]	1.01	1.02	1.02
T_m[c] (°C)	150	103	93
R_G[d] (nm)	0.7	0.9	1.6

[a] Molecular weights (M_ws) were estimated from SEC with poly(styrene) standards.
[b] M_w/M_n means molecular weight distribution.
[c] T_m means melting point.
[d] Gyration radii of the dendrimers (R_G) were estimated by molecular simulation.

3.2. Photochemical reactions of dendrimers

When *trans*-cinnamamide and its derivative are irradiated with UV light at 313 nm, the compounds typically exhibit two photochemical reactions: *trans*-to-*cis* photoisomerization and [2+2] photocycloaddition (photodimerization) [13]. As presented in

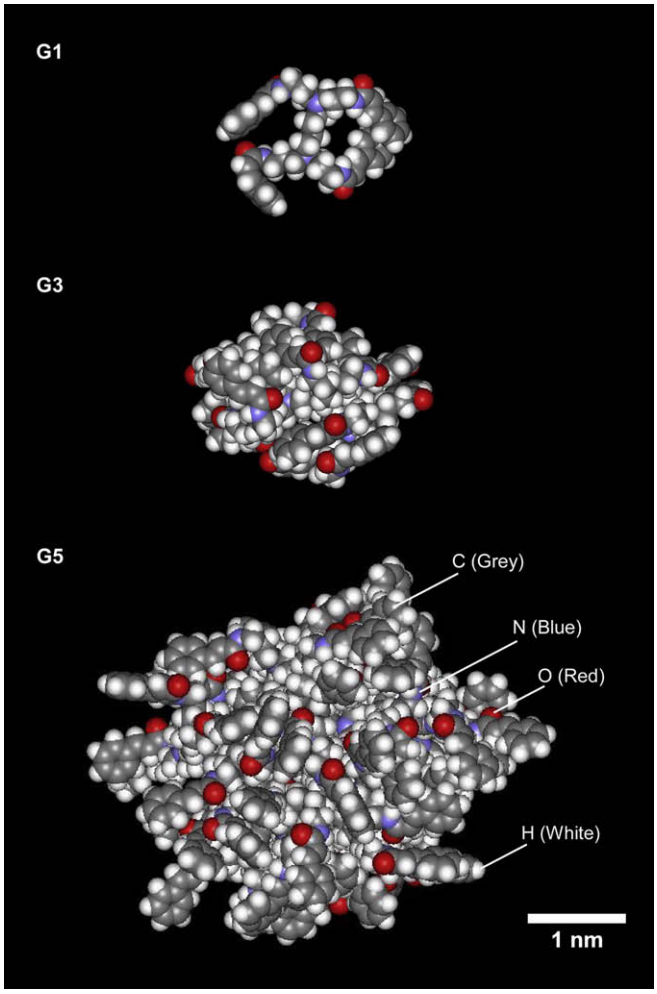

Fig. 3. Molecular models of **G1**, **G3** and **G5** optimized by computer simulation. Gray, red, blue and white parts correspond to carbon, oxygen, nitrogen and hydrogen, respectively.

Scheme 1, the *cis*-cinnamamide produced by photoisomerization is in the equilibrium state, reversibly yielding the initial *trans*-isomer, whereas [2+2] photocycloaddition is irreversible due to new cyclobutane formation between two *trans*-cinnamamide units according to Woodward–Hoffmann rule.

In this study, the photochemical behavior of the dendrimers with peripheral cinnamamides was monitored by recording the absorption spectra of the diluted dichloromethane solutions upon exposure to 313 nm light for excitation of *trans*-cinnamamide groups. Fig. 4 shows representative results of changes in absorption spectra of **G0** (*trans*-cinnamamide) and **G5** dilute solutions as a function of exposure energy of 313 nm light, respectively. The spectra of **G1** and **G3** are shown in Supplementary material (Fig. S2). All compounds were prepared at a concentration of 3.0×10^{-5} mol l^{-1} in terms of the cinnamamide unit. Before UV exposure, wavelengths at absorption maxima (λ_{max}) and spectral shape between **G0** and **G5** were similar to each other. Photoexcitation of the solutions with 313 nm light gave rise to monotonous reduction in the electronic absorption band of *trans*-cinnamamide unit from 220 to 320 nm. Such spectral changes occurred by both *trans*-to-*cis* photoisomerization and [2+2] photocycloaddition. Fig. 4(b) shows the spectra of the **G5** solution. Two isosbestic points at 245 and 315 nm could be observed at the early stage of exposure to 313 nm light, suggesting the dominant occurrence of photoisomerization. Further UV excitation over 2.0 J cm^{-2} dose brought about gradual decrease in the absorbance, accompanied by deviation from the isosbestic point at 245 nm due to photocycloaddition. In contrast, a non-dendrimer molecule of **G0** (*trans*-cinnamamide) exhibited isosbestic points during the course of UV excitation with 30 J cm^{-2} dose, as shown in Fig. 4(a). This result implies that UV excitation of the **G0** solution leads to exclusive *trans*-to-*cis* photoisomerization to attain the photostationary state. We found that photochemical behavior of **G5** is quite different from that of **G0**.

In order to obtain further insight into the photochemical behavior, we estimated the changes in the photoproduct distribution of *trans*- (f_{trans}) and *cis*-isomer (f_{cis}) and cycloadduct (f_{cyclo}) of cinnamamide groups as a function of the exposure energy of 313 nm light. From the spectral alterations, the molar fraction of photoproducts could be estimated according to the following equations [14]:

$$f_{trans} = \frac{\varepsilon_{trans}}{(\varepsilon_{trans} - \varepsilon_{cis})}\left[\frac{A}{A^0} - \left(\frac{\varepsilon_{cis}}{\varepsilon_{trans}}\right)\left(\frac{A_{iso}}{A^0_{iso}}\right)\right] \quad (3)$$

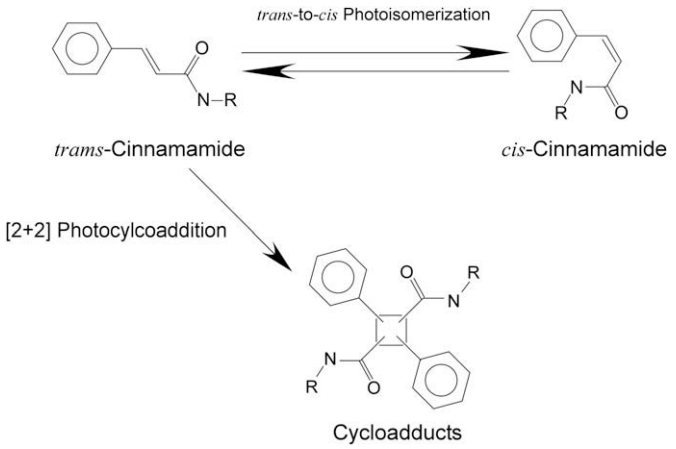

Scheme 1. Photochemical reactions of cinnamamide derivatives: *trans*-to-*cis* photoisomerization and [2+2] photocycloaddition.

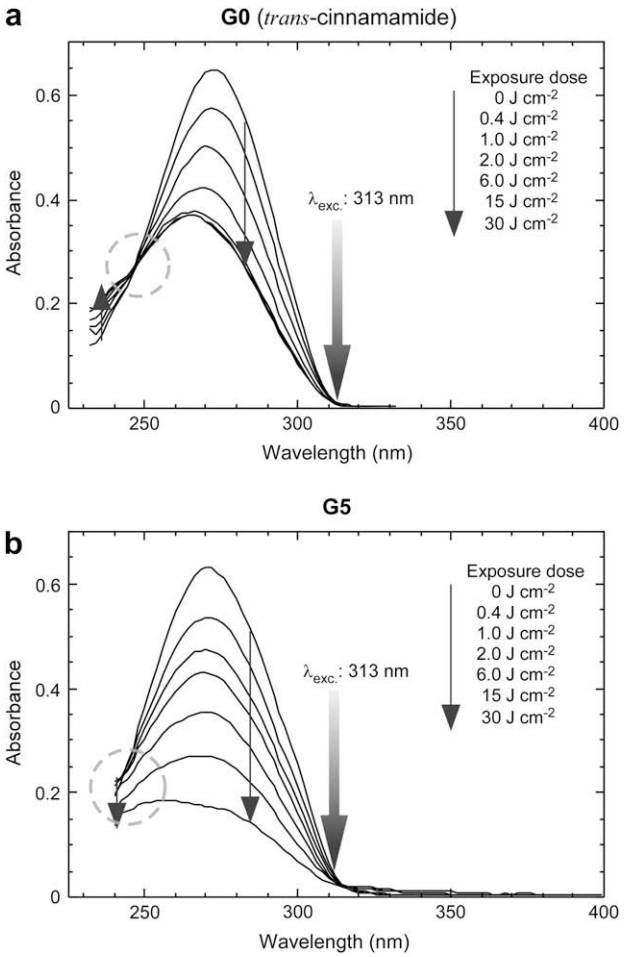

Fig. 4. Absorption spectral changes of dilute solutions of **G0** (*trans*-cinnamamide) (a) and **G5** (b) in dichloromethane upon photoexcitation with 313 nm light.

$$f_{cis} = \frac{\varepsilon_{trans}}{(\varepsilon_{trans} - \varepsilon_{cis})}\left[\frac{A_{iso}}{A^0_{iso}} - \left(\frac{A}{A^0}\right)\right] \quad (4)$$

$$f_{cyclo} = 1 - \frac{A_{iso}}{A^0_{iso}} \quad (5)$$

where ε_{trans} and ε_{cis} are the molar extinction coefficients of the *trans*- and *cis*-cinnamamides at λ_{max}, respectively. A and A_{iso} represent the absorbances at the wavelength at maximum absorption ($\lambda_{max} = 270$ nm) and at the isosbestic point ($\lambda_{iso} = 248$ nm), respectively. A^0 and $A^0{}_{iso}$ are the absorbances at the wavelengths at the initial state.

Fig. 5 shows the changes in photoproduct distribution of **G0**, **G1**, **G3** and **G5** as a function of exposure energy of 313 nm light. All compounds consumed fractions of *trans*-cinnamamide unit at early stages of UV excitation. In particular, **G0** showed quite fast rate of the *trans*-isomer consumption. This occurred from the predominant *trans*-to-*cis* photoisomerization of **G0**, resulting in negligible formation of the photocycloadduct, as shown in Fig. 5(a). In addition, we found that the rate of photocycloaddition is markedly affected by the dendrimer generation. Higher generation dendrimers gave large molar fraction of photocycloadduct [closed squares in Fig. 5(a)–(d)]. In general, [2+2] photocycloaddition of *trans*-cinnamoyl derivatives takes place at a distance of ca. 4 Å between the neighboring molecules in the crystalline solid states [13]. This fact and our observation

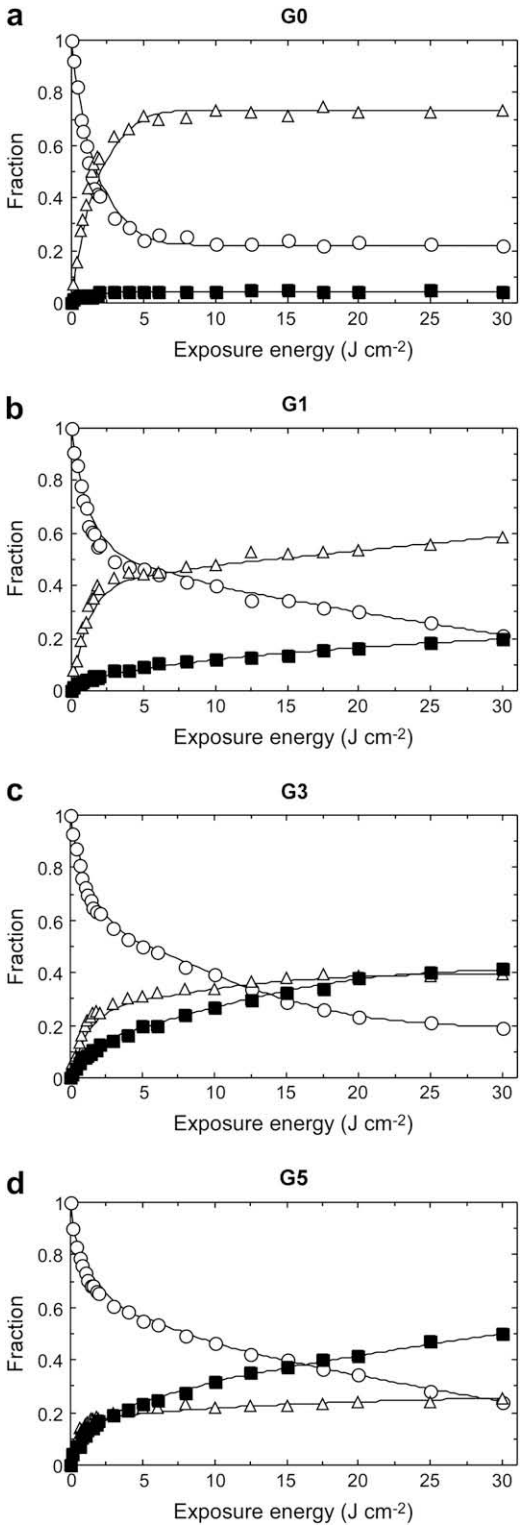

Fig. 5. Changes in photoproduct distribution of *trans*- (open circles), *cis*-isomer (open triangles) and photocycloadduct (closed squares) of cinnamamide units in **G0** (a), **G1** (b), **G3** (c) and **G5** (d) as a function of exposure energy of 313 nm light.

imply that when *trans*-cinnamamide units were attached to the peripheral surfaces of the higher generation dendrimers, photocycloaddition could be generated even in dilute solutions due to restricted molecular motion by steric crowding on the dendrimer surfaces. This is supported by the molecular models of Fig. 3.

Previously, such steric crowding behavior at molecular level has also been analyzed by fluorescence spectroscopic measurements. Crooks and Baker reported that excimer emission from ground-state dimers is observed for dilute solutions of higher generation poly(propylene imine) dendrimers covalently modified with pyrene units [11b]. It is known that pyrene or its related aromatic compounds show excimer fluorescence by overlap of π orbital at a distance of ca. 4 Å from each other [1]. Ghaddar et al. also observed excimer emission for solutions of a third-generation Frechét-type dendrimer comprising of benzylic alcohol building blocks and naphthalene peripheral groups [15]. The precedents are very consistent with our observation.

Table 2 summarizes photocycloadduct percentages of cinnamamides of **G0**, **G1**, **G3** and **G5** in various conditions after excitation with 313 nm light at a dose of 30 J cm^{-2}. In the solutions, the cycloadduct percentages were dependent on the dendrimer generation rather than the concentration. It was found that there is no remarkable difference in retention time of the dendrimers in SEC measurements before and after UV exposure, suggesting the intramolecular photocycloaddition of cinnamamide units. Similar photocycloadduct behavior was also observed for spin-coated film of cinnamamide compounds dispersed in amorphous poly(methyl methacrylate) (pMMA) matrix, as compiled in Table 2. The concentration of cinnamamide units was 9 wt% with respect to pMMA. Taking into account the precedents and our overall results, it is plausible that free volume of the chromophores modified on the outermost dendrimer surfaces is reduced by the restriction of segmental motion not only in the solutions, but also in the dispersed polymer films.

3.3. Encapsulation of phosphorescent donor in dendrimers

Pure **G1**, **G3** and **G5** show photosensitivity limited to deep ultraviolet region below 330 nm due to the absorption band of *trans*-cinnamamide units, as shown in Fig. 4 and Fig. S1. Therefore, photochemical reactions involving photoisomerization and photocycloaddition are commonly forbidden by excitation with 365 nm light. This is because there is no intrinsic absorption band of *trans*-cinnamamide around 365 nm.

In order to overcome this obstacle, we attempted encapsulation of phosphorescent donor molecules in the photoreactive dendrimer. By adding suitable organic compounds as the phosphorescent donor, the photosensitivity of *trans*-cinnamoyl units can be broaden and increased in a longer wavelength range, in which the cinnamoyl units never harvest directly. This chemical doping facilitates photoexcited non-radiative T-ET process from the triplet donor to the cinnamoyl moieties at triplet state, leading to the anticipation of more efficient photocycloaddition by irradiation with low energy [16]. In addition, typical high-generation dendrimers have the intrinsic capability to encapsulate organic dyes, metal ions and so on as guests into the nanometer cavities of the

Table 2
Photocycloadduct percentages of cinnamamides after photoexcitation with 313 nm light of 30 J cm^{-2} dose.

C (mol l^{-1})[a]	**G0**[b] (%)	**G1** (%)	**G3** (%)	**G5** (%)
6.0×10^{-6}	5	20	41	50
3.0×10^{-5}	6	22	41	50
3.0×10^{-4}	9	29	43	54
In pMMA film[c]	5	45	52	60

[a] Concentration of cinnamamides in solutions.
[b] *trans*-Cinnamamide.
[c] Cinnamamide units of 9 wt% dispersed in pMMA.

dendrimer molecules, thereby providing an isolated space to guest compounds [7].

We attempted to encapsulate 4,4′-bis(dimethyl-amino)-benzophenone (Michler's ketone; **MK**) in **G1**, **G3**, and **G3** according to the experimental procedure of a previous report [17]. **MK** was used as phosphorescent donor, because its triplet energy level (275 kJ mol^{-1}) is close to that of *trans*-cinnamoyl derivative (229 kJ mol^{-1}) [18]. It was found that both **G3** and **G5** have capability to encapsulate **MK** into the dendrimer cavities, whereas there was no **MK** molecule encapsulated in **G1**.

Fig. 6 shows absorption spectra of **G3** and **G5** with **MK**, respectively. The number of **MK** molecules encapsulated in **G3** and **G5** could be estimated from the absorption spectra with molecular extinction coefficients of *trans*-cinnamamide and **MK**. It was found that three and eight molecules of **MK** are encapsulated on the average into **G3** and **G5**, respectively. Hence, the resultant **G3** and **G5** capturing **MK** are abbreviated as **MK⊃G3** and **MK⊃G5**, respectively. Differential scanning calorimeter (DSC) measurements of both **MK⊃G3** and **MK⊃G5** revealed new endothermic peaks at 95 and 87 °C upon secondary heating, respectively, accompanied by disappearance of melting points of the pure dendrimers and **MK**. The profiles are shown in Fig. 7. The results imply good miscibility of **MK** in **G3** or **G5** without phase separation, arising from the absolute encapsulation of **MK** into the dendrimer nanocavities.

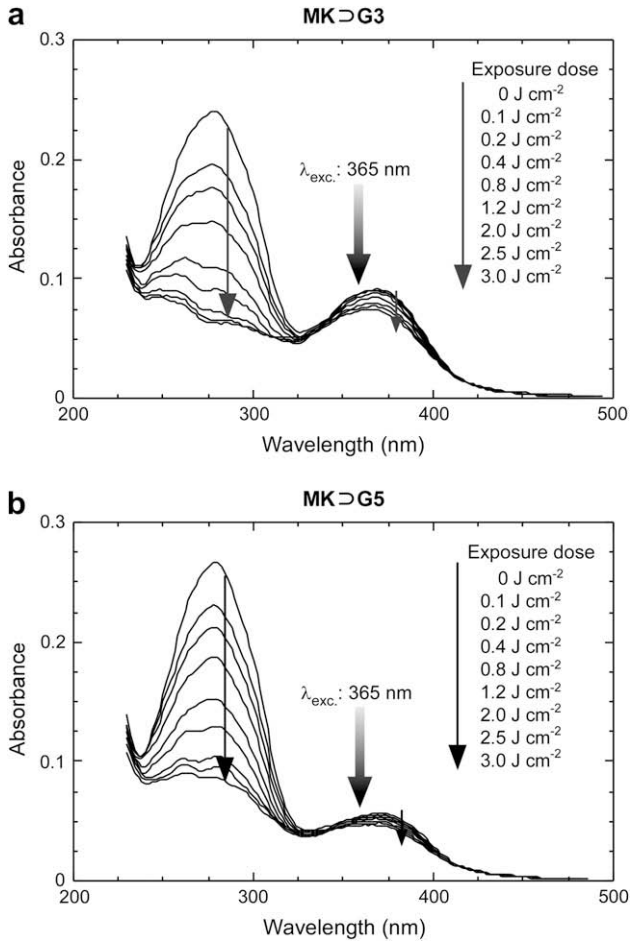

Fig. 6. Absorption spectral changes in **MK⊃G3** (a) and **MK⊃G5** (b) dispersed in pMMA film upon exposure to 365 nm light.

3.4. Triplet–triplet energy transfer in dendrimers

Fig. 6 shows the spectral changes in **MK⊃G3** and **MK⊃G5** dispersed in pMMA film upon exposure to 365 nm light, respectively. At initial state, both dendrimers exhibited two absorption bands centered at 370 and 280 nm, which are attributed to **MK** and *trans*-cinnamamides, respectively. Photoexcitation of **MK** with 365 nm light led to abrupt reduction in the band of *trans*-cinnamamide units as a result of T-ET from the **MK** donor to the peripheral *trans*-cinnamamides of dendrimers [19]. Upon prolonged exposure to 365 nm light, the absorption band of **MK** declined slightly due to the photochemical bleaching of hydrogen abstraction. By considering the photobleaching rate of **MK** (f_{MK}) in Eqs. (3)–(5), we estimated the changes in photoproduct distribution from the changes in absorption spectra as follows:

$$f_{trans} = \frac{\varepsilon_{trans}}{\varepsilon_{trans} - \varepsilon_{cis}}\left[\left(\frac{A - A^{B}}{A^{0}}\right) - \left(\frac{\varepsilon_{cis}}{\varepsilon_{trans}}\right)\left(\frac{A_{iso} - A^{B}_{iso}}{A^{0}_{iso}}\right)\right] \quad (6)$$

$$f_{cis} = \frac{\varepsilon_{trans}}{\varepsilon_{trans} - \varepsilon_{cis}}\left[\left(\frac{A_{iso} - A^{B}_{iso}}{A^{0}_{iso}}\right) - \left(\frac{A - A^{B}}{A^{0}}\right)\right] \quad (7)$$

$$f_{cyclo} = 1 - \left(\frac{A_{iso} - A^{B}_{iso}}{A^{0}_{iso}}\right) \quad (8)$$

$$f_{MK} = \frac{A_{MK}}{A^{0}_{MK}} \quad (9)$$

where A^{B}, A^{B}_{iso} and A_{MK} are absorbances at 274, 252 and 362 nm of photobleached MK by irradiation with 365 nm light, respectively. And A^{0}_{MK} is the absorbance at 362 nm before photoirradiation.

The results of photoproduct distribution are shown in Fig. 8. With regard to **MK⊃G3**, the photoisomerization of *trans*-cinnamamides leveled off at an early stage of UV exposure with 0.3 J cm^{-2} to reach 20% of *cis*-cinnamamides. On the other hand, photocycloaddition proceeded monotonously. **MK⊃G3**, in comparison to pure **G3** excited at 313 nm, consumed an eminently low energy of 365 nm to attain the photostationary state, as presented in Fig. 5(c). Additionally, the photocycloaddition rate of **MK⊃G3** was higher than that of pure **G3**. Similar photoreactive behavior could be observed for **MK⊃G5**. In order to clarify the encapsulation effect of MK in the dendrimers, we measured the absorption spectra of a simple mixture of **MK** and **G1** at their equimolar ratio. The results are shown in Supplementary material

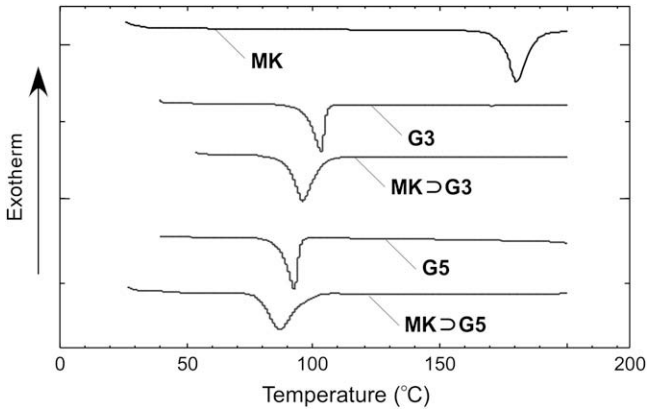

Fig. 7. DSC profiles of **MK**, **G3**, **MK⊃G3**, **G5** and **MK⊃G5**.

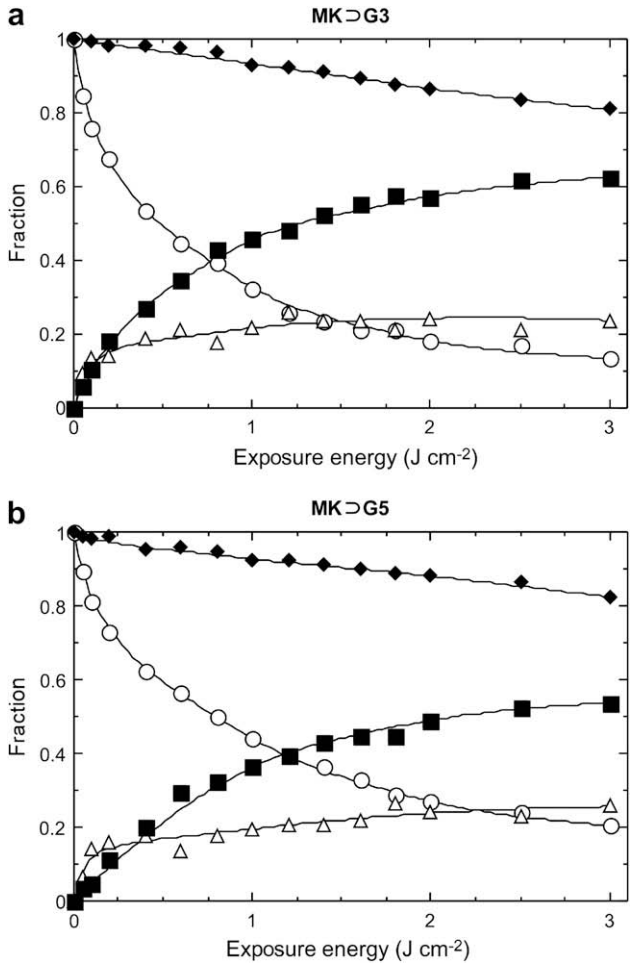

Fig. 8. Changes in photoproduct distribution of *trans*- (open circles), *cis*-isomer (open triangles) and photocycloadduct (closed squares) of cinnamamide unit and **MK** (closed diamonds) in **MK⊃G3** (a) and **MK⊃G5** (b) as a function of the exposure energy of 365 nm light.

(Fig. S3). This mixture of **MK** and **G1** exhibited the retarding behavior in the photochemical reaction rate of cinnamamide units, as compared with those of **MK⊃G3** and **MK⊃G5**, probably due to dispersion of **MK** outside of **G1**. The overall results support that the encapsulation of **MK** within the dendrimers leads to efficiently photochemical reaction of cinnamamide units. To elucidate the structural identification of dendrimer with **MK**, we measured the MALDI-TOF mass spectra of **MK⊃G3** before and after photocycloaddition. The results are shown in Fig. 9. Before UV excitation, the un-reacted **MK⊃G3** exhibited a peak at 3808 attributable to pure **G3** with potassium, probably due to desorption of **MK** from the dendrimer cavities. However, the **MK⊃G3** after photocycloaddition showed a peak at 4574, corresponding to **G3** encapsulated with three molecules of **MK**. In this way, the liberation of **MK** from the dendrimer cavities can be disabled by the photocycloaddition of dendrimers in the intramolecular way rather than the intermolecular one through the photoexcited T-ET process. The results allow us to conclude that photoexcited T-ET from **MK** in **G3** enables the intramolecular photocycloaddition of **MK⊃G3** with low UV-exposure energy and high yield.

In order to further unravel the T-ET process in the dendrimers, we measured phosphorescence spectra. Fig. 10(a) shows the changes in phosphorescence spectra of **MK⊃G3** upon exposure to 365 nm light. Before UV exposure, the phosphorescence spectrum showed a broad emission from the encapsulated **MK** at 480 nm, as

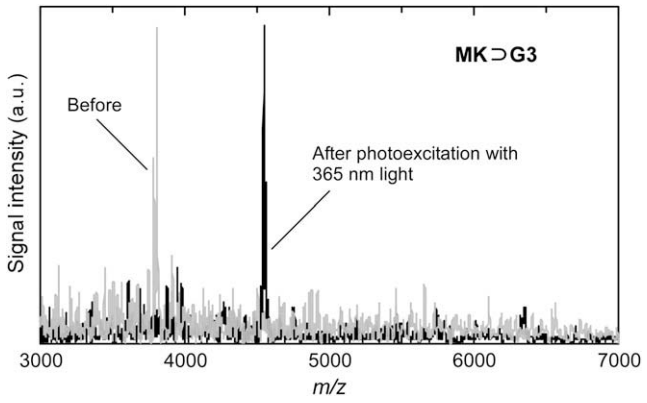

Fig. 9. MALDI-TOF mass spectra of **MK⊃G3** measured before (gray spectrum) and after photocycloaddition (black spectrum) through photoexcited triplet energy transfer process.

shown in the *Curve* **1** of Fig. 10(a) [20]. In contrast, pure **MK** dispersed in pMMA exhibited monomer emission band centered at 460 nm [18]. Such significant bathochromic shift with 20 nm in the phosphorescence maximum can be rationalized in terms of collision complex [1]. In other words, **MK** molecules interact with *trans*-cinnamamide units of **G3** in the dendrimer cavity to form the collision complex between **MK** and *trans*-cinnamamide units even at triplet excited state. Interestingly, photoexcitation with 365 nm light led to a gradual increase in the **MK** phosphorescence intensity, accompanied by bathochromic shift of the phosphorescence maximum, as a result of consumption of *trans*-cinnamamides through the photoinduced T-ET process. *Curve* **2** in Fig. 10(a) shows the phosphorescence spectrum at exposure energy with a dose of 0.8 J cm^{-2}. By prolonged UV excitation, the phosphorescence intensity was remarkably reduced at exposure doses larger than 0.8 J cm^{-2} probably due to phosphorescence quenching by the *cis*-cinnamamide and cycloadduct. More importantly, the resultant **MK⊃G3** showed an emission at 460 nm assignable to the monomer phosphorescence of **MK**, as presented in *Curve* **3** of Fig. 10(a). This result is consistent with the absorption spectral measurement that 90% of *trans*-cinnamamide is consumed at an exposure dose of 3.0 J cm^{-2}, as shown in Fig. 8(a).

The phosphorescence quenching behavior can be analyzed by using Perrin's formula, leading to the estimation of quenching radius (R_q) at which the excited **MK** is completely quenched. Perrin's formula is defined as follows [1]:

$$\ln\left(\frac{I_0}{I}\right) = \left(4\pi R_q^3/3\right)N'C \qquad (10)$$

where I_0 and I are phosphorescence intensities of **MK** without and with *trans*-cinnamamide units, respectively. N' and C correspond to the molecular number of a dissolved substance in 1.0 cm^3 and the molar concentration of *trans*-cinnamamides, respectively.

The experimental and theoretical results of **MK⊃G3** and **MK⊃G5** are shown in Fig. 10(b). **MK⊃G5** showed deviation from the theoretical Perrin relation throughout UV excitation. This can be rationalized by considering that the rate of T-ET process falls off exponentially when the molecular distance between donor and acceptor increases, according to Eq. (2).

In contrast to **MK⊃G5**, **MK⊃G3** obeyed theoretical Perrin relation of phosphorescence quenching at the early exposure stage where *trans*-cinnamamide was reduced by half. From this result, the R_q between **MK** and *trans*-cinnamamide was estimated to be ~0.5 nm. This obviously means that the present T-ET process proceeds in the nanometer-scale vicinity of the triplet excited **MK**

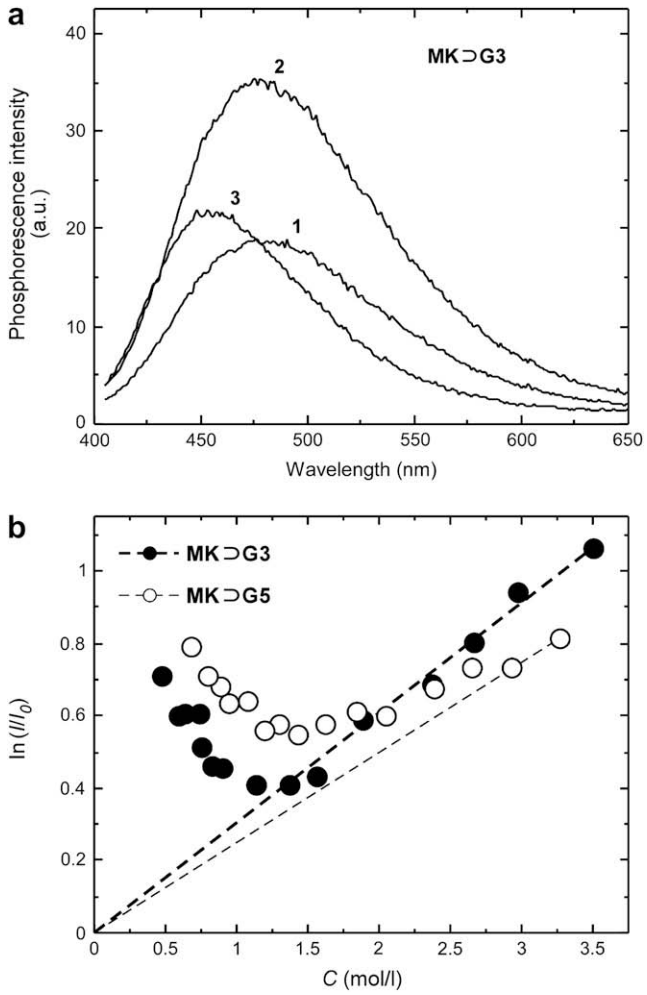

Fig. 10. (a) Changes in phosphorescence spectra of **MK⊃G3** dispersed in pMMA film upon exposure to 365 nm light. The phosphorescence spectra of **MK⊃G3** were measured before (*Curve* **1**) and after excitation with 365 nm light of 0.8 J cm^{-2} (*Curve* **2**) and 3.0 J cm^{-2} (*Curve* **3**), respectively. (b) Phosphorescence quenching profiles of **MK⊃G3** (closed circles) and **MK⊃G5** (open circles) as a function of concentration (*C*) of *trans*-cinnamamide acceptor units. Thick and thin dashed lines indicate theoretical Perrin's relationships of phosphorescence quenching of **MK⊃G3** and **MK⊃G5**, respectively.

donor. However, prolonged UV excitation brought about the deviation from Perrin's relationship due to quenching by the *cis*-cinnamamide and cycloadduct. It seems that the collision complex plays an essential role in the efficient generation of the present T-ET process in **MK⊃G3** by excitation with 365 nm light.

4. Conclusions

In conclusion, we have studied the photochemical behaviors of photoreactive poly(propylene imine) dendrimers having cinnamamide groups at the terminal positions, and found the photophysical process of photoexcited triplet–triplet energy transfer (T-ET) by encapsulating phosphorescent donors in the photoreactive dendrimer cavities. Poly(propylene imine) dendrimers were functionalized with *trans*-cinnamamide units, showing *trans*-to-*cis* photoisomerization and [2+2] photocycloaddition, at the peripheral positions. With an increase in the dendrimer generation, photocycloaddition took place preferentially by photoexcitation with 313 nm light even in dilute solutions. Such photocycloaddition behavior was strongly dependent on the dendrimer generation irrespective of the solution concentration, implying that the *trans*-cinnamamide moieties aggregate on the outermost surface of high-generation dendrimer due to restricted molecular motion by steric crowding. Moreover, the third- and fifth-generation dendrimers enabled the capture of Michler's ketone (**MK**) donors in the internal dendrimer nanocavity. As a result, efficient photocycloaddition of the *trans*-cinnamamides could be substantiated by photoexcitation with 365 nm light through T-ET from the donors. The excitation energy to reach the photostationary state was one order of magnitude smaller than that required by pure dendrimers by excitation with 313 nm light. In order to unravel the T-ET process, phosphorescence spectra were measured. By analysis with Perrin's formula, we found that the present T-ET process proceeds efficiently at ~0.5 nm vicinity of triplet excited **MK** molecules. This strategy provides us versatile clues not only to understand the T-ET process isolated in nanometer space [6d], but also to build the novel devices by the bottom-up approach [21].

Acknowledgements

The authors would like to thank for the reviewer's helpful comments. This study was carried out at the Kobe Advanced ICT Research Center (KARC) in the National Institute of Information and Communications Technology (NICT). One of the authors (S.F.) also thanks Dr. N. Shirahata of the NIMS for technical advices, and is also indebted to the partial supports from the Strategic Information and Communications R&D Promotion Programme (SCOPE) Project (No. 062103003) from the Ministry of Internal Affairs and Communications (MIC) of Japan, the Kao Foundation for Arts and Sciences, and the Yazaki Memorial Foundation for Science & Technology.

Appendix. Supplementary material

^{13}C NMR and FT-IR spectra of **G5**, absorption spectral changes of a simple mixture of **MK** and **G1**, and absorption spectral changes of dilute **G1** and **G3** upon excitation with 313 nm light are shown. Supplementary material associated with this article can be found in the online version, at doi:10.1016/j.polymer.2009.04.039.

References

[1] (a) Birks JB. Photophysics of aromatic molecules. London: Wiley-Interscience; 1970. p. 518;
(b) Turro NJ. Modern molecular photochemistry. California: University Science Books; 1991. p. 296;
(c) Klessinger M, Michl J. Excited states and photochemistry of organic molecules. Weinheim: VCH; 1995. p. 243.
[2] Kuhlbrandt W. Nature 1995;374:497–8.
[3] (a) Baldo MA, O'Brien DF, You Y, Shoustikov A, Sibley S, Thompson ME, et al. Nature 1998;395:151–4;
(b) Baldo M, Thompson ME, Forrest SR. Nature 2000;403:750–3;
(c) Wilson JS, Dhoot AS, Seeley AJA, Khan MS, Köhler A, Friend RH. Nature 2001;413:828–31;
(d) Reufer M, Walter MJ, Lagoudaksi PG, Hummel AB, Kolb JS, Roskos HG, et al. Nature Mater 2005;4:340–6.
[4] Förster T. Discuss Faraday Soc 1959;27:7–17.
[5] Dexter DL. J Chem Phys 1953;21:836–50.
[6] (a) Tomalia DA, Durst HD. Top Curr Chem 1993;165:193–313;
(b) Zeng F, Zimmerman SC. Chem Rev 1997;97:1681–712;
(c) Archut A, Azzellini GC, Balzani V, Cola LD, Vögtle F. J Am Chem Soc 1998;120:12187–91;
(d) Bosman AW, Janssen HM, Meijer EW. Chem Rev 1999;99:1665–88;
(e) Fischer M, Vögtle F. Angew Chem Int Ed 1999;38:884–905;
(f) Adronov A, Frechét JMJ. Chem Commun 2000:1701–10;
(g) Frechét JMJ. J Polym Sci A 2003;41:3713–25;
(h) Tomalia DA. Prog Polym Sci 2005;30:294–324;
(i) Puntoriero F, Nastasi F, Cavazzini M, Quici S, Campagna S. Coord Chem Rev 2007;251:536–45.
[7] (a) Jansen JFGA, de Brabander-van den Berg EMM, Meijer EW. Science 1994;266:1226–9;

(b) Cooper AI, Londono JD, Wignall G, McClain JB, Samulski ET, Lin JS, et al. Nature 1997;389:368–71;
(c) Vögtle F, Plevoets M, Nieger M, Azzellini GC, Credi A, De Cola L, et al. J Am Chem Soc 1999;121:6290–8;
(d) Chechik V, Zhao M, Crooks RM. J Am Chem Soc 1999;121:4910–1;
(e) Xu Z, Ford WT. Macromolecules 2002;35:7662–8;
(f) Zheng J, Dickson RM. J Am Chem Soc 2002;124:13982–3;
(g) Lee WI, Bae Y, Bard AJ. J Am Chem Soc 2004;126:8358–9;
(h) Yokoyama S, Otomo A, Mashiko S. Appl Phys Lett 2002;80:7–9;
(i) Otomo A, Otomo S, Yokoyama S, Mashiko S. Opt Lett 2002;27:891–3.

[8] (a) Chen J, Li S, Zhang L, Liu B, Han Y, Yang G, et al. J Am Chem Soc 2005;127:2165–71;
(b) Chen J, Li S, Zhang L, Li Y-Y, Chen J, Yang G, et al. J Phys Chem B 2006;110:4047–53.

[9] Hara M, Samor S, Cai X, Tojo S, Arai T, Momotake A, et al. J Am Chem Soc 2004;126:14217–23.

[10] The preliminary results have been published in a proceeding of The 5th International Conference on Nano-Molecular Electronics: Furumi S, Otomo A, Yokoyama S, Mashiko S. Thin Solid Films 2003;438/439:85–9.

[11] (a) Schenning APHJ, Peeters E, Meijer EW. J Am Chem Soc 2000;122:4489–95;
(b) Baker LA, Crooks RM. Macromolecules 2000;33:9034–9.

[12] Cavallo L, Fraternali F. Chem—Eur J 1998;4:927–34.

[13] Cohen MD, Schmidt GMJ. J Chem Soc 1964:1996–2000.

[14] Egerton PL, Pitts E, Reiser A. Macromolecules 1981;12:95–100.

[15] Ghaddar TH, Whitesell JK, Fox MA. J Phys Chem B 2001;105:8729–31.

[16] (a) Reiser A. Photoreactive polymers: the science and technology of resits. New York: Wiley-Interscience; 1989. p. 1;
(b) Minsk LM, Smith JG, Van Deuse WP, Wright JF. J Appl Polym Sci 1959;2:302–7.

[17] Stevelmans S, van Hest JCM, Jansen JFGA, van Boxtel DAFJ, de Brabander-van den Berg EMM, Meijer EW. J Am Chem Soc 1996;118:7398–9.

[18] Murov SL, Carmichael I, Hug GL. Handbook of photochemistry. 2nd ed. New York: Marcel Dekker; 1993.

[19] Curme HG, Natale CC, Kelly DJ. J Phys Chem 1967;71:767–70.

[20] When pure **G3** was excited with 313 or 365 nm light, there was negligible emission band. This is because *trans*-cinnamamides cannot emit phosphorescence.

[21] (a) Zimmerman SC, Wendland MS, Rakow NA, Zharov I, Suslick KS. Nature 2002;418:399–403;
(b) Beil JB, Lemcoff NG, Zimmerman SC. J Am Chem Soc 2004;126:13576–7;
(c) Love CS, Ashworth I, Brennan C, Chechik V, Smith DK. Langmuir 2007;23:5787–94;
(d) Tasdelen MA, Demirel AL, Yagci Y. Eur Polym J 2007;43:4423–30.